

SMASHING THE GUITAR: AN EVOLVING NEUTRON STAR BOW SHOCK

S. CHATTERJEE & J. M. CORDES

Department of Astronomy, Cornell University, Ithaca, NY 14853
 shami@astro.cornell.edu, cordes@astro.cornell.edu

For the Astrophysical Journal Letters

ABSTRACT

The Guitar nebula is a spectacular example of an H α bow shock nebula produced by the interaction of a neutron star with its environment. The radio pulsar B2224+65 is traveling at $\sim 800\text{--}1600\text{ km s}^{-1}$ (for a distance of 1–2 kpc), placing it on the high-velocity tail of the pulsar velocity distribution. Here we report time evolution in the shape of the Guitar nebula, the first such observations for a bow shock nebula, as seen in H α imaging with the Hubble Space Telescope. The morphology of the nebula provides no evidence for anisotropy in the pulsar wind, nor for fluctuations in the pulsar wind luminosity. The nebula shows morphological changes over two epochs spaced by seven years that imply the existence of significant gradients and inhomogeneities in the ambient interstellar medium. These observations offer astrophysically unique, *in situ* probes of length scales between 5×10^{-4} pc and 0.012 pc. Model fitting suggests that the nebula axis — and thus the three-dimensional velocity vector — lies within 20° of the plane of the sky, and also jointly constrains the distance to the neutron star and the ambient density.

Subject headings: ISM:structure—pulsars:individual (PSR B2224+65)—shock waves—stars:neutron

1. INTRODUCTION

While the steady decay of spin rates observed in radio pulsars provides a good estimate of the rate of energy loss \dot{E} , only a small fraction of the energy output of a neutron star is typically converted to directly detectable electromagnetic radiation. Most of the spindown energy loss is carried away by a relativistic wind, the properties of which are largely unknown. The best constraints on the relativistic wind derive from its interaction with the interstellar medium (ISM). This interaction has been observed, for example, in synchrotron nebulae such as the Crab Nebula (Kennel & Coroniti 1984; Gallant & Arons 1994; Melatos & Melrose 1996), where wispy structures are observed moving at $\sim 0.5c$ (Hester et al. 2002), as well as bow shocks observed in H α emission from shock-excited neutral gas around PSR B1957+20 (Kulkarni & Hester 1988) and various other pulsars (Chatterjee & Cordes 2002; Gaensler, Jones & Stappers 2002).

The Guitar nebula was discovered in deep H α imaging observations with the 5-m Hale telescope at Palomar Observatory (Cordes, Romani & Lundgren 1993). Using a model for the Galactic electron density distribution (Cordes & Lazio 2002), the dispersion measure ($DM = \int_0^D n_e ds = 35.3\text{ pc cm}^{-3}$) of PSR B2224+65 implies a distance of 1.9 kpc (hereafter parameterized as $D_{1.9}$). While the pulsar has a modest $\dot{E} = 10^{33.1}\text{ erg s}^{-1}$, the large space velocity of the pulsar ($\sim 1640 D_{1.9}\text{ km s}^{-1}$) provides the ram pressure needed to create a detectable bow shock nebula. The existence of an observable bow shock nebula also implies the presence of a significant neutral hydrogen component in the ISM near the pulsar. Here we describe Hubble Space Telescope (HST) observations of the time evolution of the nebula, and discuss the implications of the observations for our understanding of neutron star (NS) relativistic winds and the ISM.

2. HST OBSERVATIONS AND MODELING

High resolution HST observations obtained in 1994 December with the Wide Field and Planetary Camera 2

(WFPC2; Holtzman et al. 1995) have been described previously (Chatterjee & Cordes 2002). New WFPC2 observations were obtained in 2001 December, with about 2.4 times the exposure time of the earlier epoch. At both epochs, exposures were combined using variable-pixel linear reconstruction (“Drizzling”; Fruchter & Hook 2002), yielding an effective pixel scale $0''.0226$, roughly half the size of the $0''.0455$ pixels on the WFPC2 Planetary Camera chip. The H α images at the two epochs (Figure 1) were aligned to sub-pixel accuracy using eight stars (Figure 2a). The tip of the nebula has moved $1.3''$ in 7 years, consistent with the radio proper motion of PSR B2224+65 ($\mu = 182 \pm 3\text{ mas yr}^{-1}$, at a position angle $52.1^\circ \pm 0.9^\circ$; Harrison, Lyne & Anderson 1993). However, unlike the simple translation with constant shape expected for a bow shock in a uniform ambient medium, the head of the nebula has changed morphologically, showing corrugations in the limb-brightened edge as well as gaps in the H α flux, both of which vary with time.

At the tip of the nebula, the stand-off radius of the bow shock has increased over the seven-year period, as determined by model fitting (discussed below) at each epoch. Pressure balance between the relativistic NS wind and ram pressure from the ambient medium occurs at the stand-off radius,

$$R_0 = (\dot{E}/4\pi c n_A m v_*^2)^{1/2}, \quad (1)$$

where n_A is the number density of particles with mean mass m and v_* is the pulsar velocity. For the Guitar nebula, incorporating measured values for the pulsar \dot{E} and proper motion, the stand-off radius is $R_0 \approx 18 D_{1.9}^{-1} n_A^{-1/2}$ astronomical units (AU), and the predicted stand-off angle is $\theta_0 = 9.4 D_{1.9}^{-2} n_A^{-1/2}$ milliarcseconds. Bright patches appear along the edges of the nebula where it is constricted, as marked with arrows in Figure 1: the location of this brightening has moved $\sim 0.8''$ parallel to the pulsar motion along both sides of the nebula. However, in Figure 2(a), the edges perpendicular to the nebula axis have moved outwards by less than $0.3''$, remaining essentially static at several points. Meanwhile, the rear edge of H α emission

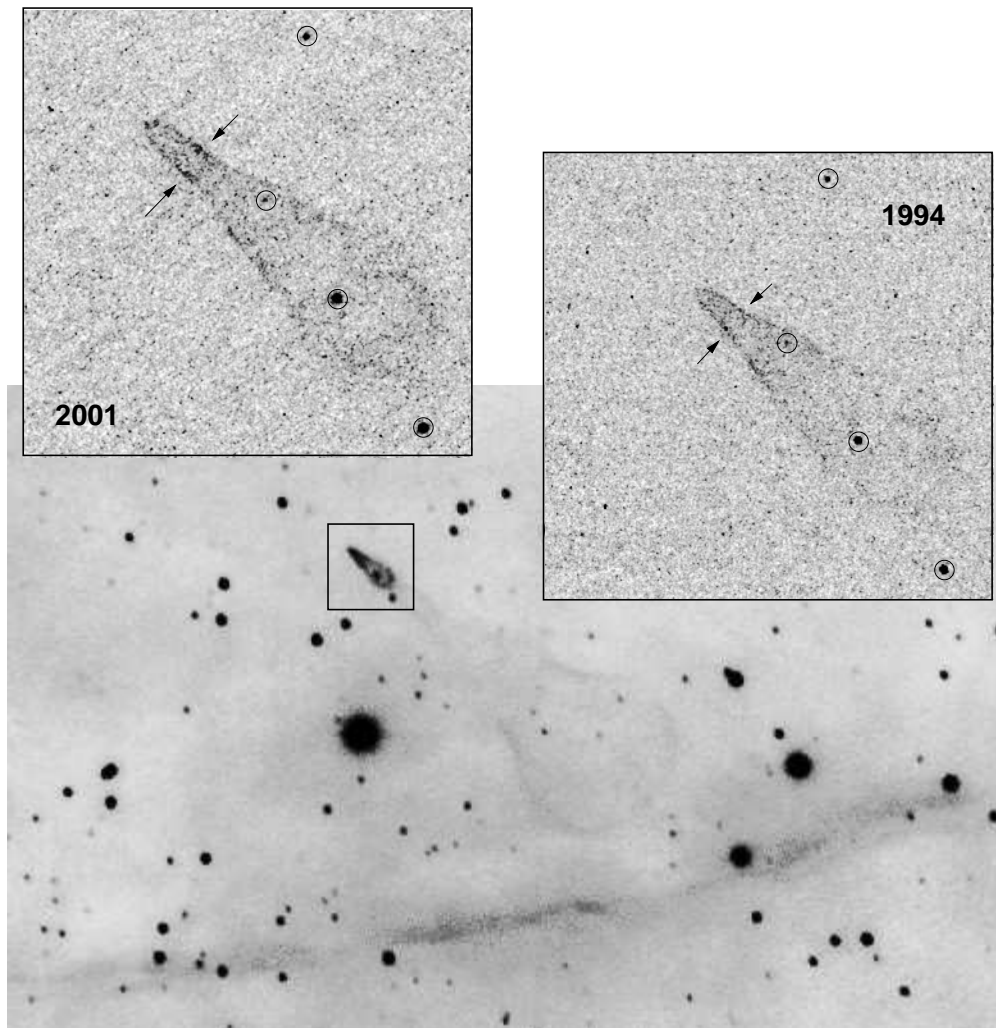


FIG. 1.— $H\alpha$ images of the head of the Guitar nebula. The bottom panel shows a wide-field image of the Guitar nebula obtained at the 5-m Hale Telescope at Palomar (Chatterjee & Cordes 2002). High resolution images of the region marked with a box ($\sim 16''$ in size) were obtained with the HST PC in 1994 (right) and 2001 (left). North is upward and east is to the left. Stars are circled, and arrows mark constricted regions in the limb-brightened $H\alpha$ emission that are conspicuously brighter (see text). Note that the neutron star is located at the very tip of the nebula at each epoch.

has actually moved backwards by $\sim 0.7''$ in 2001 compared to 1994. Possible explanations include turbulence in the shocked layers, their interaction with a complex magnetic field, or changes in any of the variables in the expression for R_0 (Equation 1), including \dot{E} . However, even for the largest observed glitches (Hobbs et al. 2002), \dot{E} changes temporarily by $\lesssim 3\%$, a negligible variation compared to the large morphological changes observed. Besides being contrary to our general understanding of spin down, a time-variable \dot{E} also fails to explain the brightening of the nebula at the locations where it appears constricted. Indeed, it is difficult to explain the evolving morphology without invoking variations in the ambient interstellar density, although instabilities in the shock structure are also possible (e.g. Draine & McKee 1993). We propose that the observations reflect the motion of PSR B2224+65 through random density inhomogeneities combined with a gradient towards a region of lower density. The bright rear edge ($\sim 11''$ downstream of the nebula tip in 1994) marks a sharp increase in density which the NS broke through ~ 70 years ago. Presently, the shock at the rear confines

the relativistic NS wind, leading to a brightening of the head of the nebula and preventing the wind from powering the rest of the Guitar body, thus producing the dim, elongated and narrow “neck” of the Guitar in Figure 1.

We argue further that the morphology of the head of the Guitar nebula is an analog for confinement by another high-density region ~ 300 years ago, which created the rounded end of the Guitar body. Fluctuations in the ambient density cause the body to be brighter where it appears constricted. In a few hundred years, as the larger Guitar body fades from view, what is currently the head of the nebula may expand to become another guitar-like structure. The scenario described here, while plausible, needs to be verified with future high-resolution monitoring observations as well as time-dependent hydrodynamic modeling of shock fronts in an ambient medium with significant density fluctuations.

Currently, in order to quantify the change in stand-off radius between epochs, we have modeled the shock front under the assumption that the nebula tip is in quasi-static equilibrium with the ambient medium. A momentum-

TABLE 1
BEST-FIT MODEL PARAMETERS FOR HST IMAGES

Epoch	Position Angle ($^{\circ}$)	Inclination † ($^{\circ}$)	Scale Factor ($D_{\text{kpc}}^{-2} n_A^{-1/2}$)	θ_0 ($''$)
1994	48 ± 2	90 ± 30	3.6 ± 1.2	0.12 ± 0.04
2001	50 ± 2	90 ± 20	4.4 ± 1.2	0.15 ± 0.04

† The fit for inclination angle was inconclusive, especially for the 1994 data, as discussed in Chatterjee & Cordes (2002).

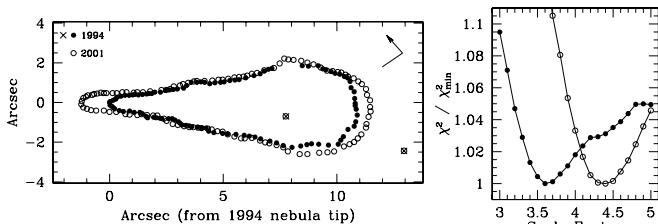


FIG. 2.— (a) Left: The outline of the limb-brightened head of the Guitar nebula in 1994 (filled circles) and 2001 (open circles), obtained by eye. The images are aligned using 8 bright stars in the PC image at each epoch: to demonstrate the image registration, two stars in the PC image section displayed in Figure 1 are marked with crosses in 1994 and open circles in 2001. (b) Right: Slices through the best fit point on the χ^2 surface for the model fit procedure on 1994 data (filled circles) and 2001 data (open circles), showing the relative change in χ^2 as a function of the scale factor $S = D_{\text{kpc}}^{-2} n_A^{-1/2}$. The implied change in ambient density at the nebula tip is $n_A(2001)/n_A(1994) \approx 0.7$.

conserving bow shock model (Wilkin 1996) was adapted to fit the $H\alpha$ emission at each epoch. The momentum-conserving description has known limitations (Bucciantini & Bandiera 2001), especially since it applies only to an ambient medium of uniform density. To avoid these problems, we restricted the model fit to within $2''.6$ of the tip of the nebula, where it is smooth and symmetric. The model is parameterized by the position angle and the inclination of the nebula to the line of sight (neither of which are expected to change significantly between epochs), the thickness of the shocked layer that emits $H\alpha$, and by a scale factor $S = D_{\text{kpc}}^{-2} n_A^{-1/2}$, which isolates the dependence of the apparent size of the nebula on distance and ambient density. Details of the model fitting procedure (for the 1994 data) are given in Chatterjee & Cordes (2002) and the best-fit parameters for both epochs (position angle, inclination, scale factor and stand-off angle) are listed in Table 1. At both epochs, the fit constrains the nebula to lie in the plane of the sky. As shown in Figure 2(b), the best-fit scale factor varies significantly between 1994 and 2001. Since the fractional change in distance to the nebula is negligible over seven years, the change in scale factor implies a decrease in ambient density by a factor ~ 0.7 (from 0.006 cm^{-3} to 0.004 cm^{-3} for $D = 1.9 \text{ kpc}$) over $1.3''$, corresponding to a length scale of $2500 D_{1.9} \text{ AU}$. The implied change in DM for density changes on this length scale is $\sim 10^{-4} \text{ pc cm}^{-3}$, which may be detectable with sensitive pulse timing observations. Additionally, the fits

establish a joint constraint on the distance to the NS and the ambient density, $D_{\text{kpc}} = 0.48 n_A^{-1/4}$. We note that the densities obtained above are low, suggesting a possible overestimate of the distance. For an ambient density of 0.05 cm^{-3} , which is comparable to the density of the local warm ionized medium (e.g. Paresce 1984), the implied distance is 1 kpc (and the height above the Galactic plane is reduced from 240 pc to 120 pc).

To check for unresolved small-scale structure in the limb-brightened nebula, the autocorrelation function was calculated for sections of the image with and without nebular emission. After accounting for Poisson noise and the contribution from smooth extended structure, the excess in the on-nebula autocorrelation function due to barely-resolved or unresolved structure (50 mas or less) is $< 5\%$ of the larger-scale nebular emission. We conclude that 50 mas represents a lower limit on the angular scale of structure in the interstellar medium probed by these HST observations of the Guitar nebula.

3. DISCUSSION

The wavenumber spectrum for electron density fluctuations in the general ISM has been delineated through a variety of measurements, including radio scintillation, scattering, pulse time-of-arrival, and Faraday-rotation, as illustrated in Figure 3. These measurements constrain the power levels in different wavenumber intervals, and suggest an overall consistency with a Kolmogorov turbulence process (Armstrong, Rickett, & Spangler 1995), although this consistency is only coarse and may be an illusion associated with the large amplitude scale of the diagram. Departures from the Kolmogorov spectrum are also inferred from pulsar scintillation measurements. The HST measurements of the Guitar Nebula provide constraints on wavenumbers not easily accessible by other probes and therefore provide a new tool for investigating fine structure in the interstellar density.

Along with the properties of the ISM, the Guitar nebula also provides a probe of the pulsar's relativistic wind. The properties of pulsar winds, including the magnetization parameter σ , the ratio of the Poynting flux to the kinetic energy flux, have been inferred primarily from the Crab nebula (Kennel & Coroniti 1984; Gallant & Arons 1994; Melatos & Melrose 1996). The existence of bow shock nebulae such as the Guitar requires collisional excitation of the neutral interstellar medium through interactions with shocked electrons and protons. These charged particles can be ejected from the NS itself, or originate

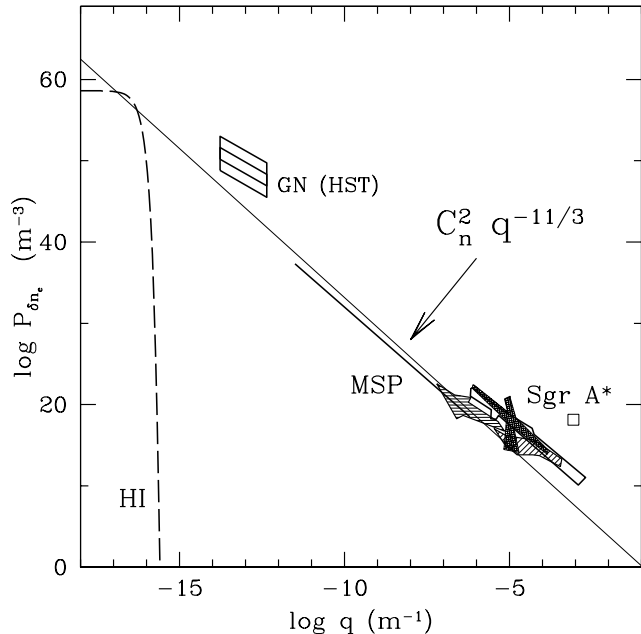


FIG. 3.— Power spectrum for electron density variations in the ISM, defined such that the integral over all wavenumbers is the mean-square electron density. The region labeled ‘GN’ designates the constraints derived from HST observations of the Guitar Nebula described here. The wavenumber range corresponds to the reciprocals of the length scales probed on angular scales between ~ 0.05 and 1.3 arcsec, assuming a distance of 1.9 kpc and a combined filling factor and ionized fraction ranging from 0.02 to 0.5 . The dashed line labelled ‘HI’ is an estimate using the length scales of standard HI clouds (McKee & Ostriker 1977), assumed to be partially ionized. The line labelled ‘MSP’ represents variations in dispersion measure for the millisecond pulsar B1937+21 (Cordes et al. 1990; Kaspi, Taylor, and Ryba 1994). The observational constraints at the highest wavenumbers result from measurements of interstellar scintillation and scattering. The point for Sgr A* represents the power level for scattering of the Galactic center source, corrected for the proximity of the scattering screen to the source (Lazio & Cordes 1998). The hatched regions incorporate constraints from scintillation and scattering observed for several hundred sources (NE2001; Cordes & Lazio 2002, and references therein). The light solid line designates a power spectrum with power-law index equal to the Kolmogorov value ($-11/3$).

from interstellar atoms through photoionization or magnetic reconnection outside the pulsar light cylinder radius ($R_{LC} = cP/2\pi$). The process by which the NS Poynting flux is converted to particle kinetic energy is not well understood: overviews of different processes are provided by Begelman & Li (1992), Gallant et al. (2002, ion loading) and Lyubarsky & Kirk (2001, striped pulsar winds). At the stand-off radius ($R_0 \gg R_{LC}$), pressure balance requires that the spindown energy of the NS be carried by the particle flux ($\sigma \ll 1$), but the shape of the nebula may encode information about the (rotation-averaged) shape of the NS wind.

Along with the Guitar nebula, future observations of the evolution of bow shock nebulae will be possible for the nearby radio-quiet neutron star RX J1856.5–3754 (van Kerkwijk & Kulkarni 2001), only ~ 120 pc away (Kaplan, van Kerkwijk & Anderson 2002; Walter & Lattimer 2002). Even at its relatively low speed (< 200 km s $^{-1}$), the neutron star travels $\sim 1''$ in a year, and evolution of the nebula should be evident on roughly this time scale.

PSR J2124–3358, a nearby millisecond pulsar with a complex bow shock nebula (Gaensler, Jones & Stappers 2002), is also promising in this regard, while the discovery of a bow shock nebula powered by the Poynting flux from a magnetar would allow investigation of the relativistic wind in the presence of an ultra-strong magnetic field.

This work is based in part on observations made with the NASA/ESA Hubble Space Telescope, obtained at the Space Telescope Science Institute, which is operated by the Association of Universities for Research in Astronomy, Inc., under NASA contract NAS 5-26555. These observations are associated with proposals 5387 and 9129. This work was also supported by NSF grants AST 9819931 and AST 0206036, and made use of NASA’s Astrophysics Data System Abstract Service and the arXiv.org astro-ph preprint service.

REFERENCES

- Armstrong, J. W., Rickett, B. J., & Spangler, S. R. 1995, *ApJ*, 443, 209
- Begelman, M. C. & Li, Z. 1992, *ApJ*, 397, 187
- Bucciantini, N. & Bandiera, R. 2001, *A&A*, 375, 1032
- Chatterjee, S. & Cordes, J. M. 2002, *ApJ*, 575, 407
- Cordes, J. M. & Lazio, T. J. W. 2002, <http://arxiv.org/abs/astro-ph/0207156>
- Cordes, J. M., Romani, R. W. & Lundgren, S. C. 1993, *Nature*, 362, 133
- Cordes, J. M., Wolszczan, A., Dewey, R. J., Blaskiewicz, M., & Stinebring, D. R. 1990, *ApJ*, 349, 245
- Draine, B. T. & McKee, C. F. 1993 *ARA&A*, 31, 373
- Fruchter, A. S. & Hook, R. N. 2002, *PASP*, 114, 144
- Gallant, Y. A. & Arons, J. 1994, *ApJ*, 435, 230.
- Gallant, Y. A., van der Swaluw, E., Kirk, J. G., & Achterberg, A. 2002, *ASP Conf. Ser.* 271: Neutron Stars in Supernova Remnants, 99
- Gaensler, B. M., Jones, D. H. & Stappers, B. W. 2002, *ApJ*, 580, L137
- Harrison, P. A., Lyne, A. G., & Anderson, B. 1993, *MNRAS*, 261, 113
- Hester, J. J. et al. 2002, *ApJ*, 577, L49
- Hobbs, G. et al. 2002, *MNRAS* 333, L7
- Holtzman, J. A. et al. 1995, *PASP*, 107, 156
- Kaplan, D. L., van Kerkwijk, M. H. & Anderson, J. 2002, *ApJ*, 571, 447
- Kaspi, V. M., Taylor, J. H., & Ryba, M. F. 1994, *ApJ*, 428, 713
- Kennel, C. F. & Coroniti, F. V. 1984, *ApJ*, 283, 694
- Kulkarni, S. R. & Hester, J. J. 1988, *Nature*, 335, 801
- Lazio, T. J. W. & Cordes, J. M. 1998, *ApJ*, 505, 715
- Lyubarsky, Y. & Kirk, J. G. 2001, *ApJ*, 547, 437
- McKee, C. F. & Ostriker, J. P. 1977, *ApJ*, 218, 148.
- Melatos, A. & Melrose, D. B. 1996, *MNRAS*, 279, 1168
- Paresce, F. 1984, *AJ*, 89, 1022
- van Kerkwijk, M. H. & Kulkarni, S. R. 2001, *A&A*, 380, 221
- Walter, F. M. & Lattimer, J. M. 2002, *ApJ*, 576, L145
- Wilkin, F. P. 1996, *ApJ*, 459, L31